Responses and impacts of atmospheric rivers to climate change

Ashley E. Payne[1] ✉, *Marie-Estelle Demory*[2], *L. Ruby Leung*[3], *Alexandre M. Ramos*[4], *Christine A. Shields*[5], *Jonathan J. Rutz*[6], *Nicholas Siler*[7], *Gabriele Villarini*[8], *Alex Hall*[9] *and F. Martin Ralph*[10]

Abstract | Atmospheric rivers (ARs) are characterized by intense moisture transport, which, on landfall, produce precipitation which can be both beneficial and destructive. ARs in California, for example, are known to have ended drought conditions but also to have caused substantial socio-economic damage from landslides and flooding linked to extreme precipitation. Understanding how AR characteristics will respond to a warming climate is, therefore, vital to the resilience of communities affected by them, such as the western USA, Europe, East Asia and South Africa. In this Review, we use a theoretical framework to synthesize understanding of the dynamic and thermodynamic responses of ARs to anthropogenic warming and connect them to observed and projected changes and impacts revealed by observations and complex models. Evidence suggests that increased atmospheric moisture (governed by Clausius–Clapeyron scaling) will enhance the intensity of AR-related precipitation — and related hydrological extremes — but with changes that are ultimately linked to topographic barriers. However, due to their dependency on both weather and climate-scale processes, which themselves are often poorly constrained, projections are uncertain. To build confidence and improve resilience, future work must focus efforts on characterizing the multiscale development of ARs and in obtaining observations from understudied regions, including the West Pacific, South Pacific and South Atlantic.

Atmospheric rivers (ARs) are synoptic-scale features characterized by their striking geometry — extending thousands of kilometres in length and an order of magnitude less in width[1] — and vertically coherent low-level moisture transport concentrated in the bottom 3 km of the atmosphere[2] (FIG. 1). In total, ARs are estimated to accomplish as much as 90% of poleward moisture transport[3,4], which, in the North Pacific, averages 700 kg m^{-1} s^{-1} (FIG. 1b), more than twice the mean annual discharge found at the mouth of the Amazon River[5]. ARs do not describe continuous moisture transport. Rather, they are continually evolving pathways that incorporate moisture from local convergence and evaporation along their track[6,7] or, in select cases, from distant source regions in the tropics or subtropics[8–12]. Owing to the complexity of their evolution, our baseline knowledge of AR characteristics at the global scale is uncertain due to the dependency on identification algorithms (BOX 1), with factors such as genesis, development and termination only recently being explored[13,14].

However, ARs are known to operate as one part of a larger, synoptic-scale dynamical system driving the poleward transport of sensible and latent heat[4,15]. They are generally found in the vicinity of extratropical cyclones. Over the North Pacific, for example, 85% of ARs are paired with extratropical cyclones[16], consistent with their observed relationship with baroclinic instabilities and the mid-latitude storm track[3,6]. However, this relationship is nuanced; only 45% of extratropical cyclones over the same region are associated with an AR[16]. Similar non-linear relationships are observed in the North Atlantic, where the evolution and life cycle of a single AR can span that of several cyclones[9]. While the phenomena are clearly related, their relationship is interactive, with potential implications on the intensification of storms and the severity of precipitation impacts on land[17,18].

Indeed, given their intense moisture transport and moist-neutrality, ARs exhibit conditions that are ideal for forced precipitation, either through interaction with topography or ascent along a warm conveyor belt or frontal boundary[19]. Thus, when ARs make landfall, they can have a range of hydrological impacts, including precipitation extremes and related hazards,

✉*e-mail:* aepayne@umich.edu

https://doi.org/10.1038/s43017-020-0030-5

Key points

- Atmospheric rivers are important components of the meridional transport of atmospheric moisture. They influence the hydroclimate of a number of regions in the mid-latitudes.
- On land, atmospheric rivers are the source of both beneficial water resources and deleterious hazards (mudslides, floods and, in their absence on longer timescales, droughts).
- The robust thermodynamic response of atmospheric moisture to climate change means that future atmospheric rivers will contain more moisture, but circulation changes and potential decreases in their precipitation efficiency must be considered in future impact studies.
- At the global scale, much is still unknown about atmospheric rivers, including basic observations of their development, their interaction with large-scale dynamics and their role in short-duration, high-volume melt events over the Arctic and Antarctic.
- Future research on the mechanisms driving atmospheric rivers and their life cycles will be a critical advancement for further quantifying their response to climate change.

as well as contributions to water supplies[20–24]. For example, ARs provide 20–30% of annual precipitation in western Europe and the western USA[22], and 14–44% of warm-season total precipitation in East Asia[25].

With 4–5 ARs present in each hemisphere at any point in time[3], their influence is felt globally. Nevertheless, AR-related impacts are largely constrained to the western coastlines of South America[26–28], South Africa[29], North America[30] and Europe[31–36], the eastern coastlines of Japan[25,37] and New Zealand[38,39], and over continental regions, such as the Central and Eastern United States[40–42]. Emerging research has also found AR-like structures over the western Mediterranean that share some characteristics with ARs in the mid-latitudes and contribute to precipitation extremes[43]. Moreover, ARs extend into the polar regions[44–47], where the increased temperatures and moisture that accompany these events further modify an environment already sensitive to feedback processes[48]. ARs, for example, have been observed to amplify summertime warming in the Arctic troposphere[49], influence the decline of Arctic sea ice by affecting the surface radiative balance[50] and bring about mass surface-melt events in West Antarctica, with the circulation patterns that accompany them[51].

Author addresses

[1]Department of Climate and Space Sciences and Engineering, University of Michigan, Ann Arbor, MI, USA.
[2]Institute for Atmospheric and Climate Science, ETH Zurich, Zurich, Switzerland.
[3]Earth Systems Analysis and Modeling, Pacific Northwest National Laboratory, Richland, WA, USA.
[4]Instituto Dom Luiz, Faculdade de Ciências, Universidade de Lisboa, Lisboa, Portugal.
[5]Climate and Global Dynamics Division, National Center for Atmospheric Research, Boulder, CO, USA.
[6]Science and Technology Infusion Division, National Weather Service Western Region Headquarters, National Oceanic and Atmospheric Administration, Salt Lake City, UT, USA.
[7]College of Earth, Ocean, and Atmospheric Sciences, Oregon State University, Corvallis, OR, USA.
[8]IIHR – Hydroscience & Engineering, The University of Iowa, Iowa City, IA, USA.
[9]Department of Atmospheric and Oceanic Sciences, University of California, Los Angeles, Los Angeles, CA, USA.
[10]Center for Western Weather and Water Extremes, Scripps Institution of Oceanography at the University of California San Diego, La Jolla, CA, USA.

Multiple factors contribute to the scale of the impacts ARs have at landfall, including duration over space and time, the temperature and intensity of moisture transport and antecedent soil moisture and snowpack conditions[52–54]. The rapid succession of individual landfalling ARs over a short period (less than a week) can supplant the initially beneficial supply of water resources. These AR 'families' are modulated by large-scale dynamics[55,56] and are most notably linked to the events leading to damage of the Oroville Dam in February 2017 (REF.[57]). Evidence of megaflood events in the palaeoclimate record in the West Coast of the United States, likely linked to landfalling AR events, suggests that the full range of their variability is still unknown[58,59].

Communities experience detrimental effects related to ARs through impacts on water resources and hazards, either primary or secondary, to extreme precipitation. The robust increase of atmospheric moisture and potential for changes in large-scale circulation with climate change have implications on the intensity, moisture sources and preferred tracks of future ARs. However, it is not enough to connect increases in the intensity of moisture transport to changes in hydrological hazards when they make landfall. The precipitation associated with ARs can respond quite differently from changes seen in moisture transport and are reliant on not only surface processes such as orographic forcing but also the location, duration and intensity of moisture transport within ARs. These changes may manifest in even more extreme AR events and exacerbate current difficulties in water management. Vital to the resilience of communities affected by ARs is knowing how their characteristics will respond to a warming climate.

In this Review, we present a comprehensive synthesis of AR responses to warming, connecting the theoretical basis for changes in ARs to results from complex models and observations. Building on theory, we first explore how thermodynamic and dynamic responses to warming affect the scale of AR impacts on land. We subsequently provide an overview of the observed and projected changes to AR characteristics, including their impacts, followed by an assessment of future research priorities. The multiple roles ARs play in the climate system and the complexity of their impacts at landfall motivate the importance of a holistic approach.

Theory-based changes to atmospheric rivers

The unique characteristics that comprise ARs provide opportunities to examine a subset of precipitation producers in a future climate from a conceptual perspective. We begin by discussing the physical theory associated with AR responses to idealized warming, focusing on their most defining feature, intense moisture transport. AR intensity is captured by the column-integrated water-vapour transport (*IVT*),

$$IVT = g^{-1}\sqrt{\left(\int_{p_s}^{p_t} qu\,\mathrm{d}p\right)^2 + \left(\int_{p_s}^{p_t} qv\,\mathrm{d}p\right)^2} \quad (1)$$

where g is standard gravity, u and v the zonal and meridional winds, respectively, q specific humidity, p_s surface pressure and p_t an upper-atmospheric reference pressure

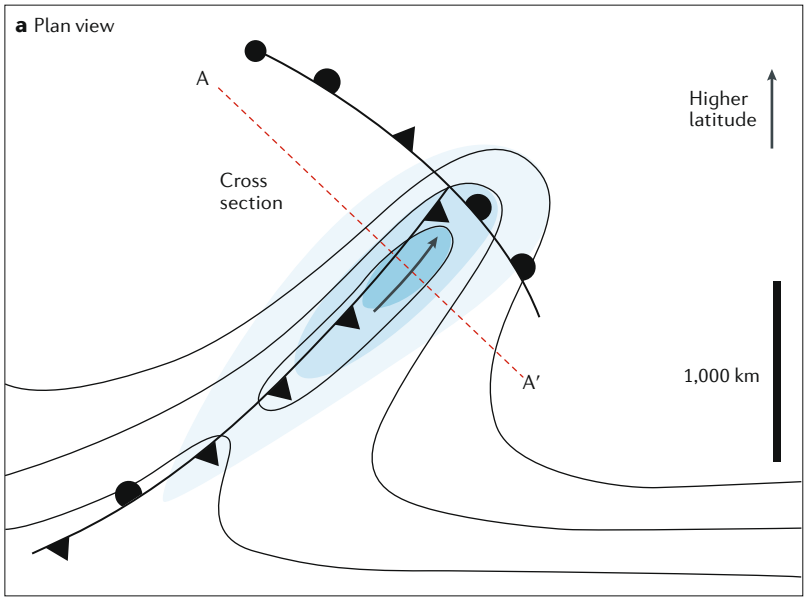

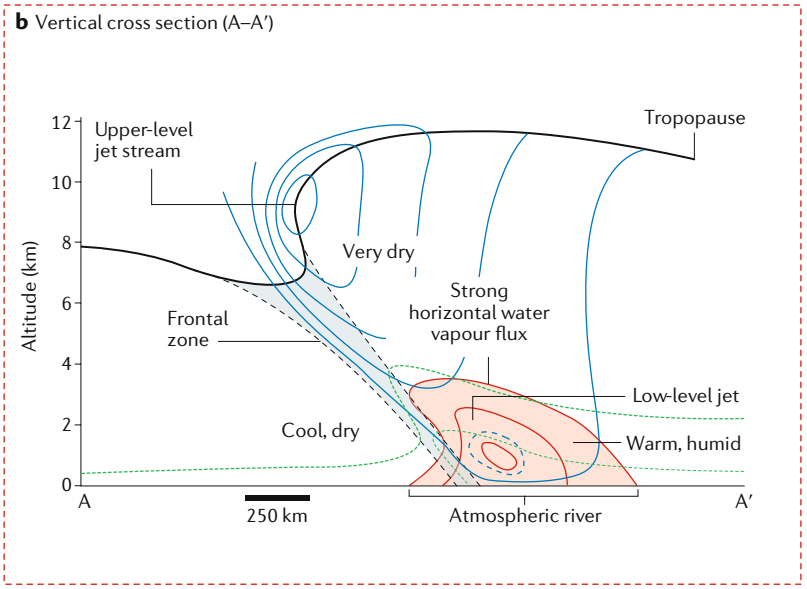

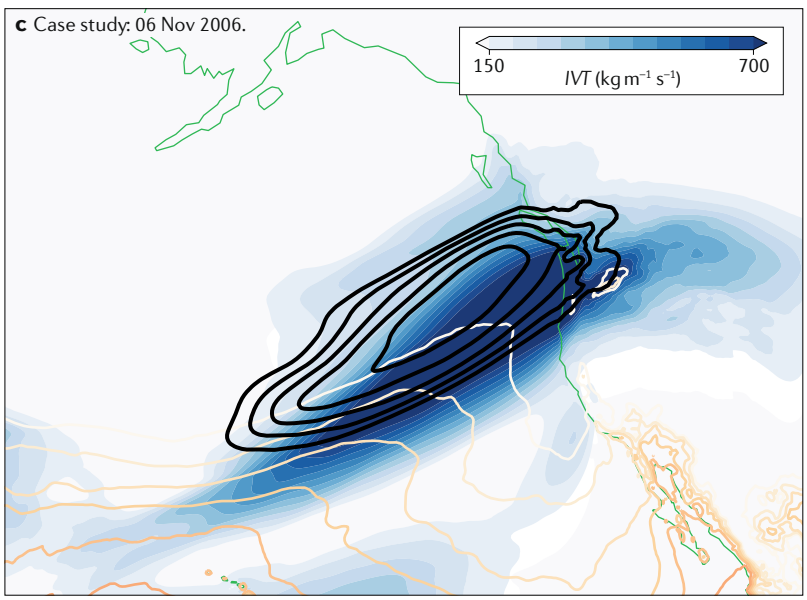

(typically set between 500 and 200 hPa). For simplicity, we define *IVT* as the magnitude of water-vapour transport, but vector definitions also appear in the literature[5]. As specific humidity changes as a function of temperature and pressure alone under saturated conditions typical of ARs, *IVT* offers a valuable investigative framework for understanding ARs. Indeed, changes in *IVT* can be decomposed into distinct contributions from thermodynamics (the change in atmospheric moisture content, q) and dynamics (the change in atmospheric motion, u and v), each of which is now discussed.

Thermodynamic responses. A natural starting point for understanding the change in the thermodynamic component of *IVT* is the Clausius–Clapeyron equation, which states that the water-vapour content of saturated air, q^*, increases nearly exponentially with temperature T according to

$$\frac{dq^*}{dT} = \alpha(T)q^*. \quad (2)$$

$\alpha(T)$ is the Clausius–Clapeyron scaling factor, defined as

$$\alpha(T) = \frac{L}{R_v T^2}, \quad (3)$$

where L is the latent heat of vaporization and R_v is the gas constant of water vapour. Within the saturated environment at the core of an AR (where $q \approx q^*$), Eq. (2) implies that the fractional change in humidity per degree of surface warming ΔT_s is approximately given by

$$\frac{1}{\Delta T_s}\frac{\Delta q}{q} = \alpha(T)\frac{\Delta T}{\Delta T_s}, \quad (4)$$

where $\Delta T/\Delta T_s$ represents the magnitude of warming at a particular height relative to the surface. At the surface, where $\Delta T = \Delta T_s$, specific humidity scales with temperature at the rate of the Clausius–Clapeyron scaling factor, $\alpha(T_s)$. This scaling is approximately 6.6% K^{-1} for surface temperatures characteristic of ARs making landfall in California in the present climate ($T_s = 13$ °C (REFS[52,60])).

Above the surface, however, the *IVT* response to warming is complicated by two factors. First, α is not constant but varies with temperature from ~6% K^{-1} in the tropical boundary layer to >7% K^{-1} at temperatures

Fig. 1 | **Characteristics of a typical atmospheric river.** **a** | A plan view of the typical structure and orientation of an atmospheric river (AR). **b** | Vertical cross section through the core of the AR (A–A′). Green contours show the water vapour mixing ratio, red contours show water vapour transport and blue contours show the wind speed. **c** | An example of a strong landfalling AR from the Pacific Northwest on 06 November 2006 in ERA5 reanalysis data. Black contours show the magnitude of vertically integrated heat flux in units of W m^{-1} co-located with the AR, drawn at intervals of 0.05×10^{11} W m^{-1}. Coloured contours depict 2-m surface temperature, drawn at intervals of 2 K. *IVT*, integrated vapour transport. Adapted with permission from REF.[5], American Meteorological Society.

Box 1 | **Identification**

Atmospheric rivers (ARs) are identifiable as transient features with extended geometry in instantaneous snapshots of daily and hourly moisture fields. However, while it is simple to separate ARs from background moisture visually, an automated method of identification becomes fundamental when understanding their behaviour over climatological timescales. To date, detection approaches have mainly been qualitative, regionally focused (particularly to the North Pacific) and subject to expert opinion. As a result, it has been challenging to compare detection algorithms.

In a future climate, the way ARs are identified is vital for diagnosing expectations of their hazards. The Atmospheric River Tracking Method Intercomparison Project (ARTMIP) is an ongoing, international effort that aims to quantify this uncertainty through the application of a variety of identification algorithms to common data sets[155,156]. Here, we explore how algorithm choice influences the month of maximum AR landfalling frequency for the western coastlines of the USA and Europe (see the figure).

The figure shows the collective agreement for algorithms across latitudes (along each coastline) and in the climatological month of maximum frequency. Identifying which locations and months are robust and which ones are not across algorithms can inform the level of uncertainty in a given analysis. This metric may be particularly important when assessing the seasonality shifts of the maximum frequency of occurrence expected to occur under global warming. While algorithms show excellent agreement in AR latitudinal distribution, this does not extend to the absolute number of ARs identified by each method. Disagreement in the total number is expected, as methodologies imposing strict requirements for AR identification detect significantly fewer ARs than those that impose less restrictive conditions. These distinctions are relevant because of their impact on metrics such as AR frequency.

Other standard AR metrics include storm intensity and duration and associated precipitation. These metrics are all somewhat dependent on methodological choices. AR intensity is particularly difficult to compare between methodologies, as most rely on intensity as a defining characteristic, and so it is slightly 'baked in' to the algorithm. For example, a method requiring that the intensity of an individual AR have a minimum value that is higher than the choice made in another algorithm will, by definition, detect stronger ARs. The value of ARTMIP is in the identification of the nuance in algorithm definitions. Moving forward, results from various ARTMIP subtopics can inform researchers on the most appropriate application for the various identification approaches.

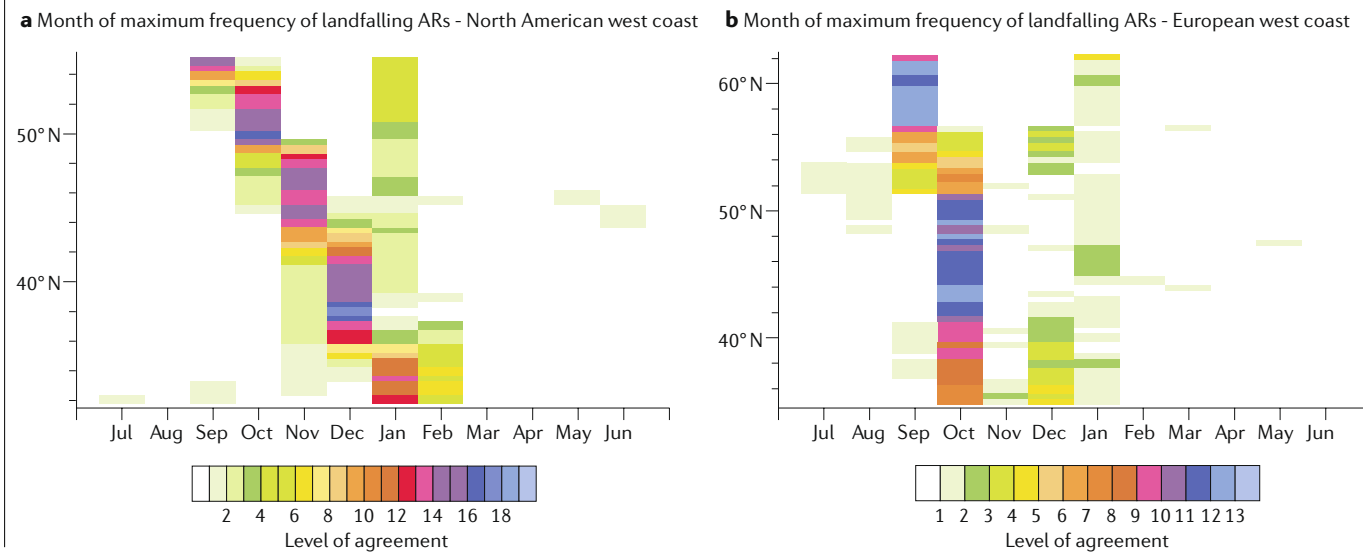

below freezing[61]. Given that temperature decreases with height, α is, therefore, larger in the upper troposphere than at the surface, amplifying the change in specific humidity (q) aloft[61]. Second, an increase in q results in more latent heat being released as saturated air ascends, in turn decreasing the lapse rate with warming and, thus, increasing ΔT with height[61–63]. Under the saturated, moist-neutral conditions of an AR, the combination of these factors implies a rate increase in column-integrated water vapour that is substantially larger than that of near-surface water vapour: 9.5% K^{-1} compared with 6.6% K^{-1} when $T_s = 13$ °C (REF.[52])). While the larger increase in *IVT* relative to surface water vapour has been described as super-Clausius–Clapeyron scaling[64], it is, in fact, a straightforward consequence of Clausius–Clapeyron scaling applied to a saturated, moist-neutral environment. Therefore, the fractional change in integrated water vapour is a reasonable approximation to the thermodynamic contribution to *IVT* change[64–66].

The vertical distribution of water vapour, wind speed and, consequently, water-vapour transport within ARs is another factor subject to change in future climate scenarios. Mid-level water-vapour transport, for example, is an important process producing heavy precipitation on the lee side of the northern Sierra Nevada[67,68]. These studies have a specific regional focus; however, the importance of mid-level transport in extending AR conditions inland of major topographic barriers can be generalized to many regions. Water vapour transported above the crest level is less likely to be lost due to forced ascent and rainout on the windward side of such barriers. Accurately modelling changes in the vertical distribution of water-vapour transport is critical to predicting future hydroclimate, particularly over interior continental regions positioned downstream of topography.

Dynamical responses. In contrast to expected thermodynamic responses, the response of atmospheric circulation to warming is much less certain[69,70]. As a consequence, our discussion of dynamical responses of *IVT* is broader and focused on two aspects that are vitally

important to the impact of ARs on land: their location of landfall and intensity. These aspects are modified by changes in the large-scale circulation patterns and by the energetics of the atmosphere.

Uncertainty in the mid-latitude-circulation response originates from the many competing influences on the location of the eddy-driven jet in a warming climate system[71]. The jet stream is the guide against which cyclones propagate and, consequently, is closely related to the location of ARs and the high *IVT* that characterizes them. In the upper atmosphere, moistening of the tropical troposphere leads to increased latent-heat release and amplified warming relative to the lower troposphere. In the lower atmosphere, declining sea ice and other feedback processes act to amplify surface-temperature increase in the polar region[72,73]. These changes have opposing effects on the meridional temperature gradient, so that the temperature gradient increases in the upper troposphere and decreases in the lower troposphere. Shifts in the eddy-driven jet with climate change depend on this 'tug-of-war' between the two responses[74] and, thereby, remains a significant source of uncertainty for diagnosing changes in precipitation patterns[75,76].

The preceding description is a much-simplified picture of the complex and interwoven mechanisms that influence the response of large-scale dynamics to warming[77]. Regional differences in the responses of the jet are certain[78]; however, generally, models show a poleward shift in the eddy-driven jet, which leads to increased static stability in the subtropics[79,80] and upward expansion of the storm track, all consistent with an increase in the upper-level meridional temperature gradient[71,81,82]. The response of the eddy-driven jet will shift future ARs poleward[66]. Those events occurring at lower latitudes may also be shifted equatorward, depending on the location and strength of the subtropical jet shift, which shows a similar poleward shift and strengthening with warming[79].

Against this simplified framework, several competing effects may influence the intensity of *IVT*. Increased atmospheric moisture with warming drives the increase of latent-heat release and, consequently, the intensification of *IVT* and associated extratropical cyclones[83]. At the same time, a reduction in the baroclinic instability due to a decrease in the meridional temperature gradient and increased efficiency of poleward moisture transport in a moister atmosphere may reduce the moisture transport[84].

The separation between potential moisture sources may influence the sources of moisture contained within ARs. Over the eastern North Pacific, while over 70% of moisture within ARs was found to be locally sourced, at least 15% was found to be subtropical or tropical in origin[85].

Precipitation responses. In climate models, there is a robust increase in global mean precipitation; however, how the response of ARs contributes towards this change is still uncertain and depends on many more factors than increased moisture alone[86]. In this section, we examine how the previously discussed thermodynamic and dynamic responses of *IVT* contribute to changes in AR-related precipitation patterns.

In regions with little topographic relief, the local precipitation rate, P, is approximately equal to the column-integrated condensation rate during a strong landfalling AR event with large *IVT*,

$$P \approx \int_0^{p_s} \omega \left.\frac{\mathrm{d}q}{\mathrm{d}p}\right|_{\theta_e} \mathrm{d}p, \tag{5}$$

where ω is the vertical velocity in pressure coordinates, $\mathrm{d}q/\mathrm{d}p$ the vertical gradient in specific humidity following a moist adiabat and θ_e the equivalent potential temperature. Given that moist-neutral stratification is a general characteristic of strong ARs, ω is not expected to change much under warming[87]. For a generally strong AR event in which ascent extends through the full depth of the troposphere, constant ω therefore implies that P will scale with warming at roughly the same rate as near-surface q (that is, $\Delta P/(P\Delta T_s) \approx \alpha(T_s)$). Consequently, precipitation from ARs will increase at a lower rate than *IVT* under warming. For example, in a comparison of the historical period to end-of-the-century Representative Concentration Pathway 8.5 (RCP 8.5) in a large ensemble of model simulations, the number of extreme-precipitation AR days increased by 28%, compared with 35% for the total number of AR days[88].

In many regions, however, orographic processes will act to enhance AR-related precipitation through interactions between the large-scale flow and local topography. In the Sierra Nevada mountain range of California, for example, windward slopes receive around four times more precipitation during ARs compared with lower elevations upstream. Similar examples of orographic-precipitation enhancement are also observed in Norway[31,89], New Zealand[39], Japan[25] and much of the western coastlines of North[90–92] and South America[27,28,93]. In these and other mountainous regions, orographic processes could strongly influence the response of AR precipitation to warming.

Recent studies have identified several mechanisms that could affect the amount and distribution of AR precipitation in mountainous regions under warming. For example, due to basic thermodynamics, the vertical structure of condensation over a mountain's windward slope will shift upward with warming, essentially requiring air to be lifted higher to reach condensation[61]. This process shifts the spatial pattern of precipitation downwind and drives a sub-Clausius–Clapeyron increase (an increase of 9.3% compared with non-orographic precipitation at 13.1%) in the total precipitation across the mountain. While regional-climate-model simulations provide some evidence of these thermodynamic effects[94,95], other changes, such as mountain-wave dynamics[96] and hydrometeor growth and fallout[63,97,98], are also thought to influence AR-precipitation responses. This complexity points to the need for further analysis of the mechanisms governing orographic precipitation and its response to climate change — an effort that will be substantially aided by greater availability of high-resolution simulations[99] (BOX 2).

Theory further suggests that an increase in water-vapour transport above crest level, as might be expected

given higher atmospheric-moisture content and a deepening troposphere, will increase the frequency with which ARs penetrate inland across significant topographic barriers[100]. Consequently, inland regions such as the western USA are anticipated to have a greater availability of atmospheric moisture. Nevertheless, this inland penetration of atmospheric moisture does not guarantee higher precipitation, given dependence on air-mass saturation (more moisture is needed to achieve this in a warmer world) and the interactions between these air masses and dynamical mechanisms that force vertical ascent[101].

The moistening of the atmosphere and the thermodynamic response of *IVT* to warming is, therefore, expected to increase precipitation related to ARs overall. Dynamic responses seem to have the largest effect on location, rather than on intensity. The poleward migration of ARs and potential modification of moisture-source regions will shift associated precipitation patterns.

Atmospheric river trends and projections

While physical theory has provided valuable insight into warming-related changes in ARs, the short duration of the satellite record and lack of observations over regions where they develop hinders the identification of trends in their behaviour. Evidence of change, therefore, exists in the form of regional case studies, trends in precipitation extremes and long-term reanalysis records.

Many studies have focused on understanding observed changes in ARs along the western coastline of North America, motivated by unprecedented hydroclimatic volatility over the last decade[102]. Here, AR activity

Box 2 | Model resolution

Over the last decade, increases in computational resources have paved the way for the improved model resolution of global climate models (GCMs). Through the intercomparison of multidecadal simulations, several high-resolution GCM campaigns have evaluated increases in spatial resolution on model performance[157–161]. However, only a few studies have shown the potential application of these GCMs for research focused on atmospheric rivers (ARs), generally when the spatial resolution is finer than 60 km globally[108,110,162–164]. In addition to better-resolved AR characteristics, increasing spatial resolution is also shown to result in more realistic climate processes, which, in turn, affect AR location, intensity and frequency of occurrence[165].

The figure shows an example of the impact of model resolution on precipitation patterns for a landfalling AR event in central Chile on 11 July 2006 (REF.[27]), simulated by three runs of the HadGEM3-GC3.1 model[166,167] at increasing spatial resolution (left to right, approximately 250, 100 and 50 km Coupled Model Intercomparison Project Phase 6 (CMIP6) nominal resolution, respectively). For comparison, each model is overlaid by daily precipitation from the same high-resolution-analysis product (NCEP Climate Forecast System (CFSv2) at 0.31° resolution) in contour (starting at 10 mm day^{-1} and increasing in increments of 10). Comparison of the three panels shows improvement in both the location and magnitude of precipitation with increasing spatial resolution, most evident in the co-location of model-simulated precipitation with the highest concentration of precipitation in CFSv2 in central Chile.

High-resolution GCMs are better able to simulate atmospheric-moisture transport over ocean basins, which contribute to increases in precipitation over land[168]. These improvements are, in part, due to better-resolved eddy-driven jet[163,169] and topography that is more realistic in both location and altitude[170]. Related to increased resolution of topography, high-resolution GCMs better capture high-impact-precipitation frequency and intensity[111,171,172]. Improvements in the vertical profile of temperature and precipitation in mountain regions are also connected to better-resolved AR impacts on the snowpack[173].

The practice of using CMIP5 models to study changes in AR characteristics needs to be critically considered, as many exist at resolutions coarser than 60 km. More research is needed to quantify where improvements in model representation are sourced, as research has shown that the impact of resolution can vary among GCMs[170]. Beyond increases in horizontal resolution, the vertical resolution of models should also be explored. For example, improvements in long-range forecasts of North Pacific AR activity at the sub-seasonal-to-seasonal scale have been made due to increased vertical resolution and a corresponding improved representation of the quasi-biennial oscillation[174,175].

Studies focusing on the impacts of resolution changes will soon be possible with the new High Resolution Model Intercomparison Project (HighResMIP[99]), for which multiple atmosphere–ocean-coupled GCMs are run over a multidecadal period, with spatial resolutions ranging between 25 km and 50 km globally, higher than those of the CMIP6 simulations. Such 'weather-resolving' GCMs will allow an examination of high-impact events in the context of climate variability and change. Retrieving information on ARs from HighResMIP would particularly benefit impact projects aiming to monitor water resources and predict flooding, such as the Advanced Quantitative Precipitation Information project over California.

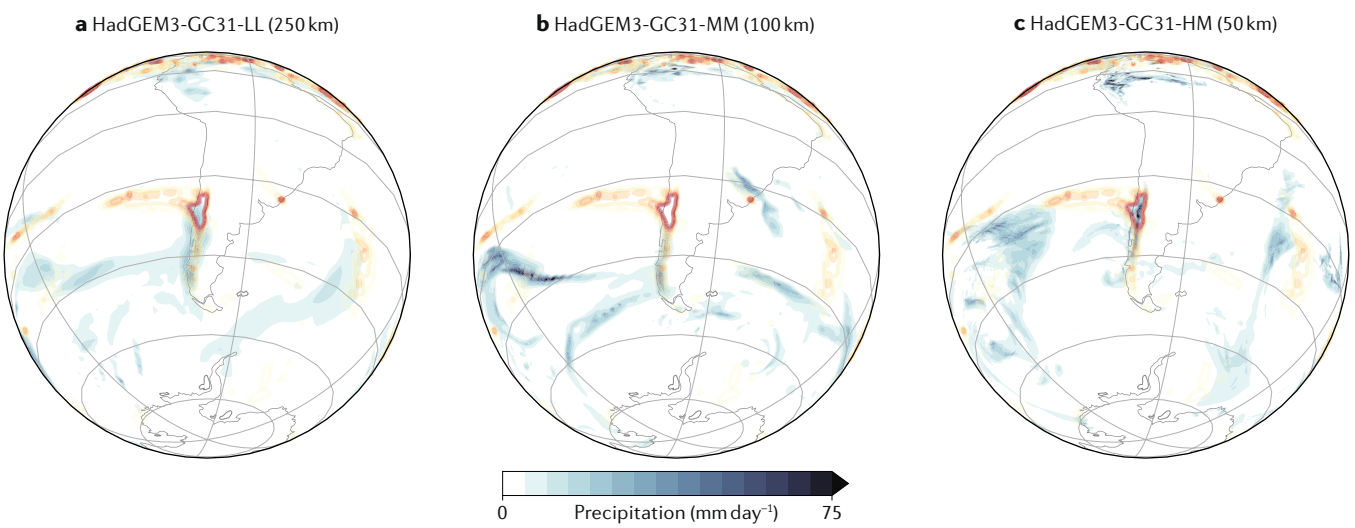

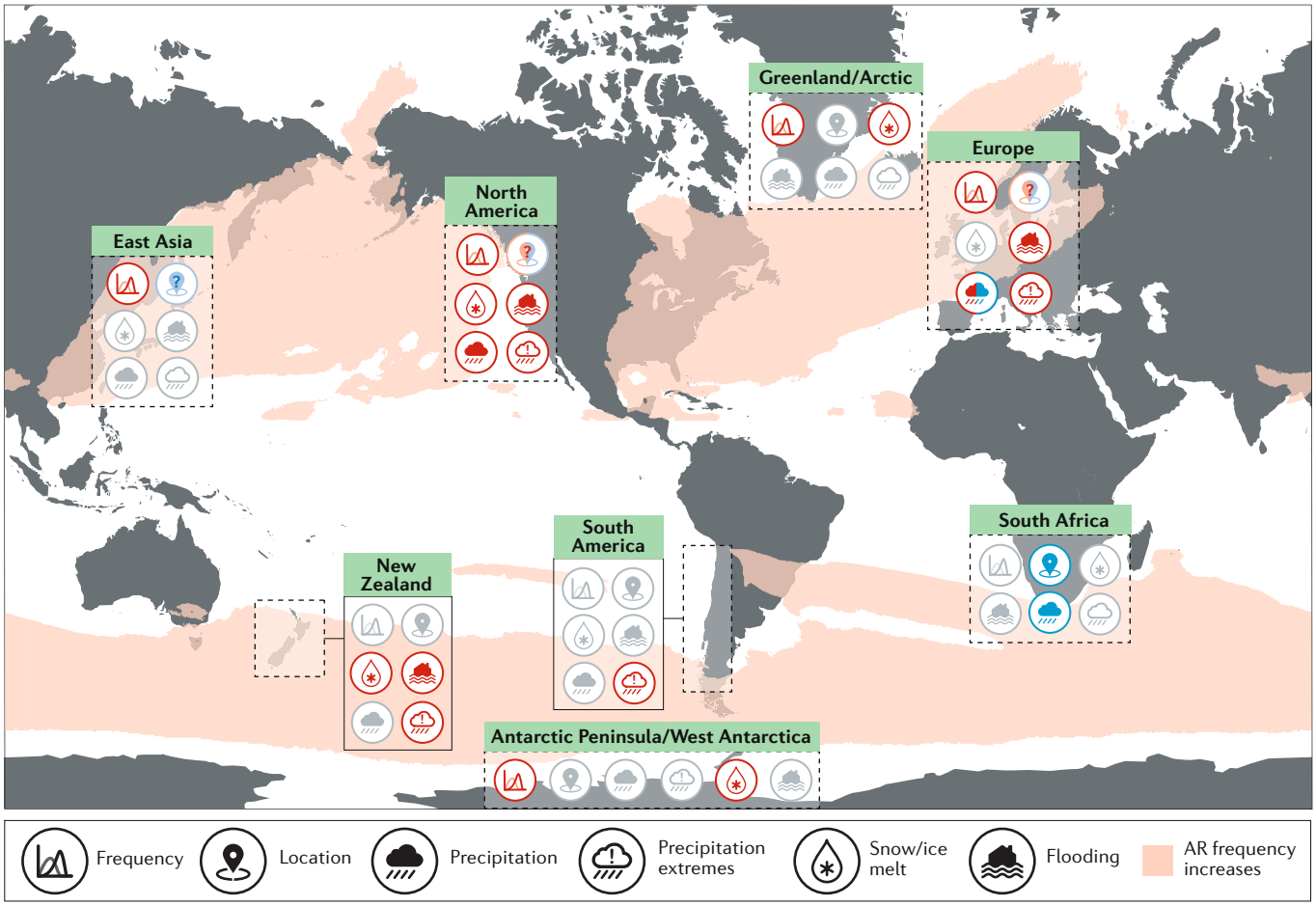

Fig. 2 | **Projected changes and impacts in atmospheric rivers.** Summary schematic of the main changes to atmospheric-river (AR) characteristics and impacts under warming. Red and blue symbols reveal increases and decreases, respectively; for frequency, red refers to a poleward movement and blue an equatorward movement of landfall. Light red and blue symbols with '?' indicate uncertainty in the projection. Grey symbols indicate unknown changes. Background shading illustrating AR frequency increases is based on Espinoza et al.[107].

has been increasing since 1948 (REFS[103,104]), possibly linked to the warming of sea-surface temperatures in the western Pacific attributable to anthropogenic climate change[105]. For instance, a 20% increase in AR days has been observed in British Columbia[106]. In addition to increased activity, the temperatures of landfalling ARs to the US West Coast have risen since the 1980s, ranging between 0.69 and 1.65 °C over the entire region, depending on season and latitude[60]. Elsewhere, understanding of observed changes is extremely limited.

Global climate models (GCMs), however, offer an opportunity to understand projections of AR characteristics (including intensity, frequency and location) in a warming climate. GCMs are excellent tools to investigate the links between ARs and the large-scale circulation, and identify the thermodynamic processes involved throughout the lifetime of ARs. To date, most projection studies have relied on simulations from the Fifth Coupled Model Intercomparison Project (CMIP5), with a horizontal grid spacing of roughly 1.5–2.5° (150–250 km). This resolution is technically high enough to detect ARs but is too coarse to capture the fine-scale features involved within ARs, including interactions with orography. An expanded discussion of the limitations of current simulations is found in BOX 2.

Globally, a comparison between the historical (1979–2002) and future (2073–2096) periods identified a 50% increase in AR frequency of occurrence — of nearly equal magnitude in the northern and southern hemispheres[107] (FIG. 2). Projections also reveal a total decrease in the total number of AR events but an increase in those events' width and length in a future climate[107]. It should be noted, however, that those increases may be an artefact of the increases in *IVT* with warming.

Many studies also use GCMs to examine the regional characteristics of ARs in a warming climate[11,34,52,64,66,88,108–113]. In Europe, for example, the number of AR days is anticipated to increase by 127–275% under RCP 8.5 (REF.[64]) when comparing 1974–2004 to 2070–2099. Similarly, along the western coast of the USA, the frequency of *IVT* days above the historical 99th percentile is projected to increase by up to 290% over the same time period[113], consistent with the projected increases shown elsewhere[109,110]. A summary of these regional changes is shown in FIG. 2 and TABLE 1, revealing the high degree of uncertainty or absent information

Table 1 | **Summary of atmospheric river responses to warming**

Study	Frequency	Location	Precipitation	Precipitation extremes	Flooding	Snow/ice melt
North America						
Curry et al.[149]	–	–	–	–	↑	–
Dettinger[52]	↑	–	–	–	–	–
Dominguez et al.[154]	↑	–	–	–	–	–
Espinoza et al.[107]	↑	–	–	–	–	–
Gao et al.[64]	↑	–	–	–	–	–
Gershunov et al.[103]	–	–	↑	–	–	–
Gershunov et al.[177]	–	–	–	↑	–	–
Gonzales et al.[60]	–	–	–	–	↑	–
Hagos et al.[88]	↑	–	–	↑	–	–
Islam et al.[148]	–	–	–	–	↑	–
Mahoney et al.[100]	–	–	↑	–	↑	–
Mallakpour et al.[178]	–	–	–	–	↑	–
Payne and Magnusdottir[108]	↑	↑↓	–	–	–	–
Pierce et al.[179]	↑	–	–	–	–	–
Polade et al.[114]	–	–	–	↑	–	–
Shields and Kiehl[110]	↑	↑↓	–	–	–	–
Singh et al.[150]	–	–	↑	–	↑	↑
Swain et al.[102]	–	–	–	↑	–	–
Radić et al.[109]	↑	↑	↑	↑	–	–
Warner et al.[113]	↑	–	↑	↑	–	–
East Asia						
Kamae et al.[25]	–	–	↑*	–	–	–
Kamae et al.[162]	↑	↓	–	–	–	–
South America						
Loikith et al.[180]	–	–	–	↑	–	–
Valenzuela and Garreaud[93]	–	–	–	↑	–	–
Viale and Nuñez[26]	–	–	↑*	–	–	–
New Zealand						
Kingston et al.[38]	–	–	–	↑*	↑*	–
Little et al.[39]	–	–	–	–	–	↑*
South Africa						
Blamey et al.[29]	–	–	↑*	–	–	–
Sousa et al.[112]	–	↓	↓	–	–	–
Europe						
Espinoza et al.[107]	↑	–	–	–	–	–
Gao et al.[66]	↑	↓	↑	↑	–	–
Lavers et al.[32]	–	–	–	↑*	–	–
Lavers et al.[33]	–	–	–	↑*	–	–
Lavers and Villarini[34]	–	–	↑*	↑*	–	–
Pasquier et al.[181]	–	–	–	↑	–	–
Ramos et al.[11]	↑	–	–	–	–	–
Shields and Kiehl[110]	↑	–	–	–	–	–
Sousa et al.[115]	–	↑	↑UK and ↓Iberia	–	–	–

Table 1 (cont.) | **Summary of atmospheric river responses to warming**

Study	Frequency	Location	Precipitation	Precipitation extremes	Flooding	Snow/ice melt
Antarctic Peninsula/West Antarctica						
Bozkurt et al.[46]	–	–	–	–	↑*	–
Gorodetskaya et al.[44]	–	–	–	↑*	–	–
Wille et al.[51]	–	–	–	–	↑*	–
Greenland/Arctic						
Hegyi and Taylor[50]	–	–	–	–	↓*	–
Lavers et al.[182]	–	–	–	–	–	–
Mattingly et al.[183]	↑*	–	–	–	↑	–

References for the material included in FIG. 2 to summarize the responses and impacts of atmospheric rivers to warming. Upward-facing arrows indicate increases and downward-facing arrows indicate decreases. Asterisks next to arrows indicate where changes are uncertain, but where observational precedent exists.

outside of the western coastlines of North America and Europe.

FIGURE 3 shows a comparison of thermodynamic (left column) and dynamic (right column) responses of *IVT* to warming. The calculations use data from a high-resolution data set of historical simulations and RCP 8.5 projections of the end of the 21st century. The panels show the dominance of thermodynamic changes over those from dynamics, in line with results from the UK and the western coastline of North America[64,65,108,110,113].

Also revealed, however, is the uncertainty in diagnosing dynamical responses due to biases in the mean position of the jet in the CMIP5 models[64]. As discussed previously, dynamical changes are most discernible at lower latitudes, where the projected expansion of the subtropics and the poleward shift of the jet have the most influence. For example, in Mediterranean climate zones of the lower mid-latitudes, poleward shifts in the storm track are projected to also shift the distribution of AR landfalls, resulting in a decrease in both the amount and frequency of winter precipitation[66,114,115]. One exception is California, where many GCMs predict a southward migration of the mid-winter storm track caused by an El Niño-like shift in climatological sea-surface temperatures[108,110]. This effect is partly compensated in the annual mean by poleward storm-track changes in the spring and fall[64]. Significantly, even in most of the Mediterranean climates that are affected by storm-track shifts, the strongest ARs are still projected to intensify at roughly the Clausius–Clapeyron rate expected from thermodynamics alone[114]. Combined with a decrease in total precipitation in these regions, this result implies a substantial increase in precipitation volatility, characterized by an increase in the frequency of both wet and dry extremes[108,110,114,116]. In addition to an increase in sub-seasonal variability, CMIP5 models projected a sharpening of the seasonal cycle of AR frequency in California that contributes to a sharpening of the seasonal cycle of extreme precipitation in the region, with important implications for floods and fire hazards[117].

Impacts of atmospheric rivers on land

Hydrological impacts. The interaction of topography with the intense moisture transport found in ARs generally tie them to substantial hydrological impacts when they make landfall. These impacts are primarily felt through influences on water resources and through precipitation-related hazards, such as floods and landslides. Indeed, ARs have both beneficial and destructive characteristics, as indicated by a recently developed AR scale that quantifies the transition from beneficial precipitation and fewer hazards (AR categories 1–2) to heavy precipitation and numerous hazards (AR categories 4–5)[54]. Here, we discuss the observed hydrological impacts of ARs.

On the global scale, ARs contribute approximately 22% of the global run-off, reaching 50% in certain regions[118]. The western coast of the USA is one such region, where the visibility of AR impacts has resulted in a wealth of hazard-related literature summarized in FIG. 2 and TABLE 1. Here, ARs are associated with numerous wintertime extreme-precipitation events, which, in turn, have been connected to riverine flooding. For instance, ARs have been found to control the upper tail of peak flood-frequency distribution[119] and account for 80–90+% of the annual maximum peak discharge in 1,375 long-term stream gauges[120]. In the Russian River, northern California, all seven floods that exceeded the monitor stage between 1997 and 2006 were further linked to ARs[121], as were 46 of 58 annual maximum flood peaks in four basins in western Washington[122]. The impacts of ARs are not limited to riverine flooding; 40–60% of annual sea-level maxima at several sites along the West Coast were also connected to AR storm events[123].

The effects of ARs also extend beyond the western coast of the USA, albeit with decreasing (yet hydrologically important) magnitudes. For example, in semi-arid north-eastern Arizona, ARs dominate heavy precipitation events, explaining 64–72% of precipitation exceeding the 98th percentile. This excess rainfall contributes to rain-on-snow events, increased run-off and 45% of annual maximum flows to inland basins[124]. Over the central part of the USA, ARs are further found to account for 20–70% of the heaviest daily precipitation extremes and more than 70% of flood events[125], including catastrophic floods in the Midwest in June 2009 (REF.[126]) and in Tennessee in May 2010 (REF.[127]).

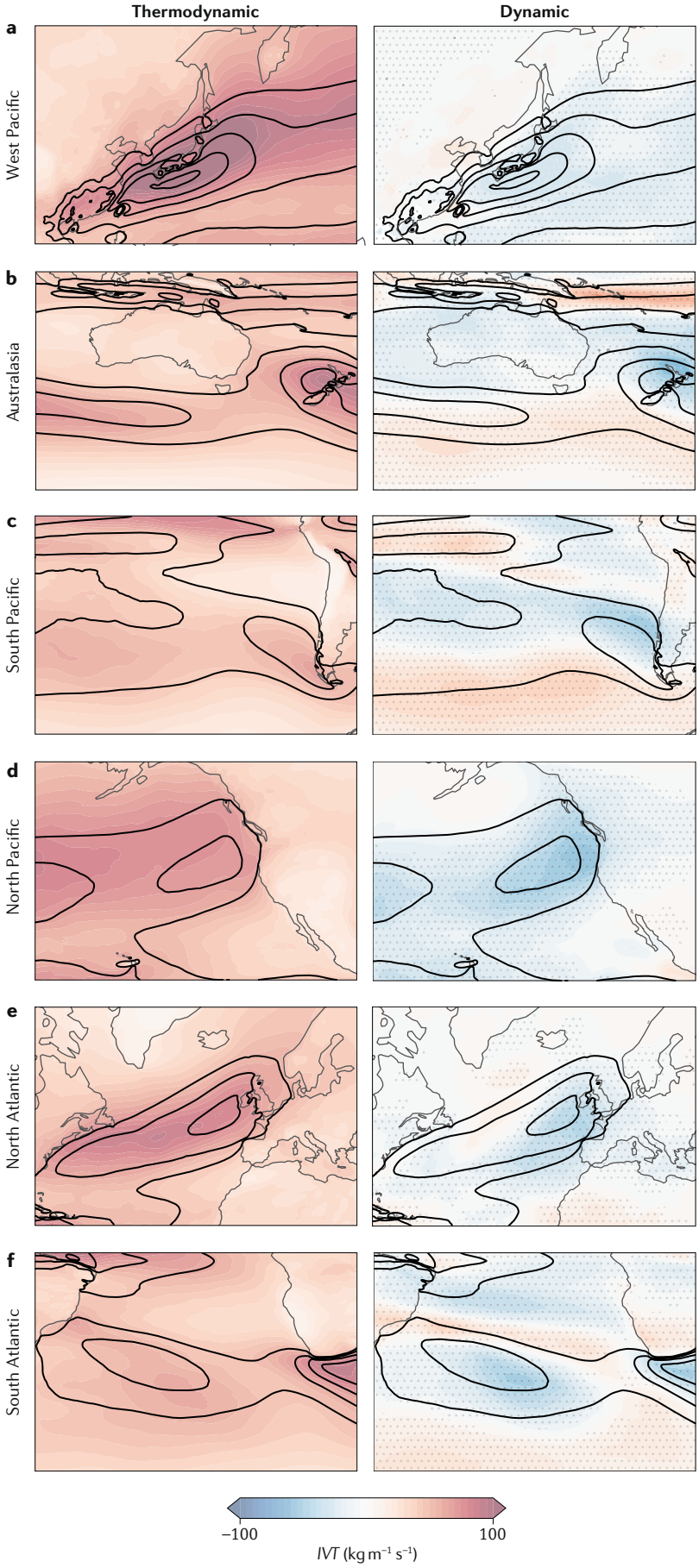

Fig. 3 | **Decomposition of integrated vapour transport.** Thermodynamic (left column) and dynamic (right column) responses to warming for the West Pacific (part **a**), Australasia (part **b**), South Pacific (part **c**), North Pacific (part **d**), North Atlantic (part **e**) and South Atlantic (part **f**). The panels show the average response over all available Atmospheric River Tracking Method Intercomparison Project (ARTMIP) catalogues that participated in the Tier 2 project based on high-resolution (0.25°, 3-hourly) climate-change simulations from the International CLIVAR C20C+ Detection and Attribution project[176]. A full list of algorithms included in this figure can be found in the supplementary material. Stippling in the right column indicates agreement in the sign of the change between 80% of algorithms. There is no disagreement in the sign of the change in the thermodynamic response, so stippling is not shown in the left column. The historical climatology of integrated vapour transport (*IVT*) for landfalling atmospheric rivers is illustrated in black contours (contours starting at 200 kg m^{-1} s^{-1} and increasing in intervals of 50). The decomposition methodology follows that of REF.[64], in which *IVT* is rescaled so that the left column shows the change in moisture between Representative Concentration Pathway 8.5 (RCP 8.5) and the historical period, and the right column shows the change in winds between RCP 8.5 and the historical period.

In the south-east, as much as 41% of non-summer heavy-precipitation events (above 100 mm day^{-1}) are connected to ARs[41]. In addition to precipitation impacts, hazards related to ARs also manifest in damaging winds, with the majority of insurance losses in excess of 1 billion USD linked to ARs[23].

ARs are further associated with precipitation extremes over much of western Europe, where observations show the importance of topography for driving precipitation from landfalling events[22]. Compared with what is observed in the western USA, AR-related impacts reach far inland in western Europe. Broadly, ARs contribute up to 30% of precipitation, but exact distributions are sensitive to seasonal variability[22]. Over the UK, ARs are a dominant contributor to wintertime precipitation extremes (50% compared with only 20% in the summer months) and floods[32]. In a study of nine different river basins, for example, 40–80% of flood events were associated with persistent ARs[33]. Similarly, over Norway, ARs contribute 56 of 58 of the most extreme daily-precipitation events[128] and also tied to costly flood events over that region[31]. Over the Iberian Peninsula, the association with ARs is more nuanced, with a clear zonal gradient in the importance of their landfall to precipitation extremes[35]; some studies indicate a weak relationship between summertime precipitation extremes and ARs[17], whereas others reveal that ARs still play a significant role in the summertime, at least in Portugal, explaining 9 of 10 precipitation extremes between 1950 and 2007 (REF.[129]).

Elsewhere, the influence of ARs has been studied comparatively less. However, evidence suggests that 80% of days with heavy precipitation conditions (46 days total) over the central Andes are attributable to AR conditions[26]. Here, AR events are distinguished from other precipitation-producing phenomena by an increase in the intensity of moist upslope flow,

producing rainfall accumulations that are more than twice those for non-AR conditions[27,28]. South African wintertime precipitation has been further linked to persistent AR activity, with approximately 70% of the top 50 daily-precipitation extremes experienced during AR events[29]. ARs have also been documented to impact the hydrology of East Asia; ARs account for between 14% and 44% of precipitation falling during the extended summer over Taiwan, southern China, the Korean Peninsula, and central and western portions of Japan[25].

ARs frequently contribute to compound events (the combination of multiple climate drivers that contribute to societal or environmental risks and which may increase in the future[130]), particularly when heavy precipitation occurs together with or in close succession to other natural hazards. Specifically related to ARs are their ties to precipitation extremes and warm, moist air. For example, in October 2011 in the Bernese Alps of Switzerland, the combined effect of a heavy snowfall event followed by the passage of an AR resulted in a rapid increase of temperatures and melting of snowpack[131]. The resultant flooding of the valley below had costly impacts on the infrastructure and security of that region. In California, several studies have connected post-fire debris flows[132] and landslides[133] to the incidence of landfalling ARs, either in their interaction with water-resistant wildfire burn scars or by saturation of the soil. The potential for secondary hazards that outweigh the initial impact of ARs is also possible.

Despite the hazardous effects of ARs, they can also be beneficial by providing precipitation that is essential for water supply and resources[52]. Over the west coast of the USA, for example, ARs are thought to provide an average of 30–50% of annual precipitation[52,90] and have been responsible for ending 33–74% of droughts in the region[134], including the persistent California drought from 2012 to 2016 (REF.[135]). Indeed, it has been determined that, in regions currently frequented by ARs, the recurrence of droughts would increase by up to 90% in the absence of ARs[118], due to both the immediate precipitation responses and the longer-term persistence of soil moisture after the event itself[136].

ARs are significant contributors to the snowpack, and, hence, water resources in regions where snow makes up a substantial fraction of the water supply year-round. For example, ARs contribute between 30–40% of the total season accumulation of snow water equivalent (SWE) across the Sierra Nevada[90]. Unlike non-AR events that build the snowpack over multiple storms throughout the cold season, as few as 1–2 extreme AR-related snowfall events dominate contributions to SWE in the Sierra Nevada. In contrast, ARs making landfall in the US Pacific Northwest produce average gains in SWE given topographical differences and a subsequent larger fraction of rain[30].

Because of their warmer temperatures, ARs disproportionately contribute to rain-on-snow events that increase the ratio of streamflow to precipitation[137,138]. In general, snowpack ablates more during AR than non-AR events because of the higher temperatures, but increased long-wave radiation also plays a secondary role[139]. The importance of rain-on-snow events in contributing to run-off is demonstrated by the significant increase of the run-off-to-precipitation ratio with (74%) and without (43%) pre-existing snowpack during AR landfall in the western USA[139]. Overall in the western USA, ARs explain 30–60% of the variability of annual run-off and sharpen the seasonality of water-resources availability in the west coast mountain watersheds by reducing the fraction of winter precipitation that accumulates as snowpack on April 1st[139]. In Europe, by contrast, rain-on-snow events are not as well documented. Nevertheless, limited case studies exist, such as in the Bernese Alps, Switzerland, where an AR event on 10 October 2011 caused substantial damage due to flooding[131].

Trends in projected impacts. Given the substantial hydrological impacts of ARs in the present climate, and the projected changes in AR characteristics expected in the future, in this section, we outline how precipitation processes and impacts may also change. In many mountainous regions influenced by landfalling ARs, warming is expected to alter hydrological regimes and water resources. Increases in the ratio of rainfall to snowfall during the wet season will increase the likelihood of wintertime flooding[140]. With warmer temperatures, the timing of the peak snowmelt occurs earlier in the cold season, which has the effect of reducing streamflow in late spring or early summer[141–143]. Contraction of the snowmelt season towards winter and early spring reduces the energy available for melt, which can lead to a reduction in the snowmelt rate, with potential implications for streamflow, soil moisture and ecosystems[144].

Climate change may further exacerbate the impacts of AR storms on the snowpack and rain-on-snow events. However, the visibility of any trends is highly dependent on climatological temperatures[145], which, in turn, depend on the surface elevation. This nuance is apparent in high-resolution regional-climate simulations, which project less frequent rain on snow at lower elevations (a decrease of between 2 and 20 days $year^{-1}$), but the opposite at higher elevations (an increase of between 2 and 10 days $year^{-1}$) in the western USA[146]. At lower elevations, similar projections show a decline in the snowpack, which reduces the chance of the coexistence of rainfall and snow[146]. However, warming has less of an effect on snowpack at higher elevations, while a shift from snowfall to rainfall may enhance the chance of rain on snow. These same simulations also indicate an increase of flood risk between 20% and 200%, with the most considerable changes found in high-altitude mountains, including the Sierra Nevada, the Colorado River headwaters and the Canadian Rocky Mountains. It should be noted that the studies reviewed here do not isolate AR-induced versus non-AR-induced changes. However, the fact that rain-on-snow events happen more under AR conditions suggests that the projected changes in rain on snow are relevant. These results motivate a more in-depth analysis of changes in snowpack, rain on snow and flooding in the future.

The winter of 2016–2017 was an extremely wet year in California, with record extreme precipitation

associated with an abnormally high number of intense ARs making landfall[57]. Probing the hydrological conditions of this wet year with and without historical and future warming, land-surface-model simulations show that historical warming has already reduced the Sierra Nevada SWE by 20% and increased early-season run-off by 30%[147]. Snowpack loss will continue under future warming, resulting in a more extreme run-off related to a smaller snow-to-rain ratio, rather than to increased snowmelt[144,146]. Altogether, historical warming has already exacerbated extreme run-off in the Sierra Nevada in the above-normal AR winter of 2016–2017 (REF.[57]). Under future warming, similar winter conditions suggest an even larger increase in flood risk.

Investigations of projected impacts specific to ARs are scarce but are consistent with the more general review summarized above. British Colombia's Fraser River is an example of a mid-latitude basin influenced by nearby topography and by ARs. By the end of the 21st century under RCP 8.5, peak flow in this basin is increasingly decoupled from springtime snowmelt due to the decline in winter snowpack, and, instead, coupled to AR-related precipitation extremes[148]. Further work suggests that the increased frequency and intensity of projected ARs affecting this basin manifests as more frequent and larger wintertime flows, and an increase in the likelihood of flooding[149]. Similar results were found on the Salt River and Verde River basins in Arizona[150]. Compared with the present, ARs affecting middle and high elevations in the Pacific Northwest are expected to result in more liquid than solid precipitation, potentially exacerbating the flood risk[100].

Summary and future perspectives

In this Review, we have identified key AR characteristics that are likely to change with anthropogenic warming. Our focus here has been to connect ongoing theoretical research on precipitation extremes with knowledge of ARs. Within a theoretical framework, future ARs are expected to carry more moisture, though moisture increases do not necessarily translate to increases in moisture transport, as storm-track changes and jet shifts also play a role. Areas with elevated terrain are most susceptible to increases in precipitation extremes attributable to ARs; however, in the absence of topography, effects are expected to scale in line with Clausius–Clapeyron[61] and thermodynamic responses (FIG. 2). Projections further reveal increases in frequency and a general poleward shift in landfall location. When combined with enhanced atmospheric moisture and warmer temperature, the hydrological impacts of ARs may also be exacerbated (FIG. 3).

Despite a strong theoretical basis for understanding AR projections in the future, simulations of sufficient resolution to represent AR processes remain limited. Circulation drivers that modulate AR landfall location and duration, for example, are vital to understanding AR impacts on land[151], but are a key source of uncertainty. Dynamic contributions to changes in *IVT* are much smaller, but may increase in importance in the transition regions between the expanding subtropics and the mid-latitudes. Uncertainty in projecting changes in the transition regions is strongly tied to uncertainty in projecting changes in tropical circulation and high-latitude processes, pointing to the fundamental challenge in modelling convection and cryosphere processes, respectively, in Earth-system models.

Given their importance to water resources, the ability to forecast AR impacts at extended ranges is essential, especially when factoring in the relatively long timescales needed for resource mobilization. Regions that rely on ARs for the replenishment of reservoirs and snowpack can feel their absence just as much as their presence. However, questions remain about the processes that contribute to their evolution before landfall, limiting forecasting capabilities. Thus, increased understanding of such processes — including diabatic effects of ARs on downstream weather-system development[17] — is rapidly needed to improve prediction and, thereby, water-resource management. It is well known that current models do not accurately represent the effects of latent-heat release[83]. Given the projected increases in atmospheric moisture and, therefore, in *IVT* related to ARs, there is an urgent need to better understand how they interact with large-scale circulation. This insight is particularly relevant in understanding the interactive feedbacks between ARs and cyclone intensification[83], which have implications on their precipitation signatures on land.

Although ARs are beneficial water resources, they can also have devastating and costly effects on human populations. An emerging area of research focuses on the intersection between the physical and human-related impacts associated with ARs. In the US West Coast, for example, flood damages linked to even a small increase in AR intensity can translate to large economic losses[152]. The interrelation between human activities, such as expansion of human development[153] and modification of surface processes, means that new approaches are needed to communicate AR impacts. Model frameworks that bridge physical impacts with economic costs and policy development can be useful in this regard[154]. Similar approaches are needed to pass scientific understanding to stakeholders, such as water managers and policymakers, especially for weather extremes that are projected to worsen in the future.

AR characteristics over the North Pacific and impacts to the US West Coast serve as a test bed for the development of our knowledge of their impacts and variability. FIGURE 3 reveals robust understanding of the changes and impacts in this region, but an absence of understanding or high degree of uncertainty elsewhere. For instance, South America, South Africa and East Asia are strongly impacted by ARs, but our knowledge here is highly constrained by inadequate observational networks or field campaign data, as well as lack of model validation. Exploration of ARs at the global scale, therefore, represents the next frontier, including the high latitudes where analysis is urgently needed, given links to surface melt and glacial mass balance. Global and region-specific catalogues from the many ARTMIP subprojects represent an excellent resource for this work.

Published online 9 March 2020

1. Newell, R. E., Newell, N. E., Zhu, Y. & Scott, C. Tropospheric rivers? – A pilot study. *Geophys. Res. Lett.* **19**, 2401–2404 (1992).
2. American Meteorological Society. *Atmospheric River. Glossary of Meteorology*. http://glossary.ametsoc.org/wiki/Atmospheric_river (2019).
3. Zhu, Y. & Newell, R. E. A proposed algorithm for moisture fluxes from atmospheric rivers. *Mon. Weather Rev.* **126**, 725–735 (1998).
4. Newman, M., Kiladis, G. N., Weickmann, K. M., Ralph, F. M. & Sardeshmukh, P. D. Relative contributions of synoptic and low-frequency eddies to time-mean atmospheric moisture transport, including the role of atmospheric rivers. *J. Clim.* **25**, 7341–7361 (2012).
5. Ralph, F. M. et al. Dropsonde observations of total integrated water vapor transport within North Pacific atmospheric rivers. *J. Hydrometeorol.* **18**, 2577–2596 (2017).
6. Cordeira, J. M., Ralph, F. M. & Moore, B. J. The development and evolution of two atmospheric rivers in proximity to western North Pacific tropical cyclones in October 2010. *Mon. Weather Rev.* **141**, 4234–4255 (2013).
7. Dacre, H. F., Clark, P. A., Martínez-Alvarado, O., Stringer, M. A. & Lavers, D. A. How do atmospheric rivers form? *Bull. Am. Meteorol. Soc.* **96**, 1243–1255 (2015).
8. Bao, J.-W., Michelson, S. A., Neiman, P. J., Ralph, F. M. & Wilczak, J. M. Interpretation of enhanced integrated water vapor bands associated with extratropical cyclones: their formation and connection to tropical moisture. *Mon. Weather Rev.* **134**, 1063–1080 (2006).
9. Sodemann, H. & Stohl, A. Moisture origin and meridional transport in atmospheric rivers and their association with multiple cyclones. *Mon. Weather Rev.* **141**, 2850–2868 (2013).
10. Garaboa-Paz, D., Eiras-Barca, J., Huhn, F. & Pérez-Muñuzuri, V. Lagrangian coherent structures along atmospheric rivers. *Chaos* **25**, 063105 (2015).
11. Ramos, A. M., Tomé, R., Trigo, R. M., Liberato, M. L. R. & Pinto, J. G. Projected changes in atmospheric rivers affecting Europe in CMIP5 models. *Geophys. Res. Lett.* **43**, 9315–9323 (2016).
12. Hu, H. & Dominguez, F. Understanding the role of tropical moisture in atmospheric rivers. *J. Geophys. Res. Atmos.* **124**, 13826–13842 (2019).
13. Zhou, Y., Kim, H. & Guan, B. Life cycle of atmospheric rivers: identification and climatological characteristics. *J. Geophys. Res. Atmos.* **123**, 12715–12725 (2018).
14. Guan, B. & Waliser, D. E. Tracking atmospheric rivers globally: spatial distributions and temporal evolution of life cycle characteristics. *J. Geophys. Res. Atmos.* **124**, 12523–12552 (2019).
15. Shields, C. A. et al. Meridional heat transport during atmospheric rivers in high-resolution CESM climate projections. *Geophys. Res. Lett.* **46**, 14702–14712 (2019).
16. Zhang, Z., Ralph, F. M. & Zheng, M. The relationship between extratropical cyclone strength and atmospheric river intensity and position. *Geophys. Res. Lett.* **46**, 1814–1823 (2019).
17. Eiras-Barca, J. et al. The concurrence of atmospheric rivers and explosive cyclogenesis in the North Atlantic and North Pacific basins. *Earth Syst. Dyn.* **9**, 91–102 (2018).
18. Dacre, H. F., Martínez-Alvarado, O. & Mbengue, C. O. Linking atmospheric rivers and warm conveyor belt airflows. *J. Hydrometeorol.* **20**, 1183–1196 (2019).
19. Ralph, F. M., Neiman, P. J. & Rotunno, R. Dropsonde observations in low-level jets over the northeastern Pacific Ocean from CALJET-1998 and PACJET-2001: mean vertical-profile and atmospheric river characteristics. *Mon. Weather Rev.* **133**, 889–910 (2005).
20. Rutz, J. J., Steenburgh, W. J. & Ralph, F. M. Climatological characteristics of atmospheric rivers and their inland penetration over the western United States. *Mon. Weather Rev.* **142**, 905–921 (2014).
21. Guan, B. & Waliser, D. E. Detection of atmospheric rivers: evaluation and application of an algorithm for global studies. *J. Geophys. Res. Atmos.* **120**, 12514–12535 (2015).
22. Lavers, D. A. & Villarini, G. The contribution of atmospheric rivers to precipitation in Europe and the United States. *J. Hydrol.* **522**, 382–390 (2015).
23. Waliser, D. & Guan, B. Extreme winds and precipitation during landfall of atmospheric rivers. *Nat. Geosci.* **10**, 179–183 (2017).
24. Ridder, N., de Vries, H. & Drijfhout, S. The role of atmospheric rivers in compound events consisting of heavy precipitation and high storm surges along the Dutch coast. *Nat. Hazards Earth Syst. Sci.* **18**, 3311–3326 (2018).
25. Kamae, Y., Mei, W. & Xie, S.-P. Climatological relationship between warm season atmospheric rivers and heavy rainfall over East Asia. *J. Meteorol. Soc. Japan Ser. II* **95**, 411–431 (2017).
26. Viale, M. & Nuñez, M. N. Climatology of winter orographic precipitation over the subtropical central Andes and associated synoptic and regional characteristics. *J. Hydrometeorol.* **12**, 481–507 (2011).
27. Garreaud, R. Warm winter storms in central Chile. *J. Hydrometeorol.* **14**, 1515–1534 (2013).
28. Viale, M., Valenzuela, R., Garreaud, R. & Ralph, F. M. Impacts of atmospheric rivers on precipitation in southern South America. *J. Hydrometeorol.* **19**, 1671–1687 (2018).
29. Blamey, R. C., Ramos, A. M., Trigo, R. M., Tomé, R. & Reason, C. J. C. The influence of atmospheric rivers over the South Atlantic on winter rainfall in South Africa. *J. Hydrometeorol.* **19**, 127–142 (2018).
30. Neiman, P. J., Ralph, F. M., Wick, G. A., Lundquist, J. D. & Dettinger, M. D. Meteorological characteristics and overland precipitation impacts of atmospheric rivers affecting the West Coast of North America based on eight years of SSM/I satellite observations. *J. Hydrometeorol.* **9**, 22–47 (2008).
31. Stohl, A., Forster, C. & Sodemann, H. Remote sources of water vapor forming precipitation on the Norwegian west coast at 60°N – a tale of hurricanes and an atmospheric river. *J. Geophys. Res. Atmos.* **113**, D05102 (2008).
32. Lavers, D. A. et al. Winter floods in Britain are connected to atmospheric rivers. *Geophys. Res. Lett.* **38**, L23803 (2011).
33. Lavers, D. A., Villarini, G., Allan, R. P., Wood, E. F. & Wade, A. J. The detection of atmospheric rivers in atmospheric reanalyses and their links to British winter floods and the large-scale climatic circulation. *J. Geophys. Res. Atmos.* **117**, D20106 (2012).
34. Lavers, D. A. & Villarini, G. The nexus between atmospheric rivers and extreme precipitation across Europe. *Geophys. Res. Lett.* **40**, 3259–3264 (2013).
35. Ramos, A. M., Trigo, R. M., Liberato, M. L. R. & Tomé, R. Daily precipitation extreme events in the Iberian Peninsula and its association with atmospheric rivers. *J. Hydrometeorol.* **16**, 579–597 (2015).
36. Brands, S., Gutiérrez, J. M. & San-Martín, D. Twentieth-century atmospheric river activity along the west coasts of Europe and North America: algorithm formulation, reanalysis uncertainty and links to atmospheric circulation patterns. *Clim. Dyn.* **48**, 2771–2795 (2017).
37. Hirota, N., Takayabu, Y. N., Kato, M. & Arakane, S. Roles of an atmospheric river and a cutoff low in the extreme precipitation event in Hiroshima on 19 august 2014. *Mon. Weather Rev.* **144**, 1145–1160 (2016).
38. Kingston, D. G., Lavers, D. A. & Hannah, D. M. Floods in the Southern Alps of New Zealand: the importance of atmospheric rivers. *Hydrol. Process.* **30**, 5063–5070 (2016).
39. Little, K., Kingston, D. G., Cullen, N. J. & Gibson, P. B. The role of atmospheric rivers for extreme ablation and snowfall events in the Southern Alps of New Zealand. *Geophys. Res. Lett.* **46**, 2761–2771 (2019).
40. Lavers, D. A. & Villarini, G. Atmospheric rivers and flooding over the central United States. *J. Clim.* **26**, 7829–7836 (2013).
41. Mahoney, K. et al. Understanding the role of atmospheric rivers in heavy precipitation in the southeast United States. *Mon. Weather Rev.* **144**, 1617–1632 (2016).
42. Mo, R. & Lin, H. Tropical–mid-latitude interactions: case study of an inland-penetrating atmospheric river during a major winter storm over North America. *Atmosphere-Ocean* **57**, 208–232 (2019).
43. Lorente-Plazas, R. et al. Unusual atmospheric-river-like structures coming from Africa induce extreme precipitation over western Mediterranean Sea. *J. Geophys. Res. Atmos.* **125**, e2019JD031280 (2020).
44. Gorodetskaya, I. V. et al. The role of atmospheric rivers in anomalous snow accumulation in East Antarctica. *Geophys. Res. Lett.* **41**, 6199–6206 (2014).
45. Woods, C., Caballero, R. & Svensson, G. Large-scale circulation associated with moisture intrusions into the Arctic during winter. *Geophys. Res. Lett.* **40**, 4717–4721 (2013).
46. Bozkurt, D., Rondanelli, R., Marín, J. C. & Garreaud, R. Foehn event triggered by an atmospheric river underlies record-setting temperature along continental Antarctica. *J. Geophys. Res. Atmos.* **123**, 3871–3892 (2018).
47. Turner, J. et al. The dominant role of extreme precipitation events in Antarctic snowfall variability. *Geophys. Res. Lett.* **46**, 3502–3511 (2019).
48. Nash, D., Waliser, D., Guan, B., Ye, H. & Ralph, F. M. The role of atmospheric rivers in extratropical and polar hydroclimate. *J. Geophys. Res. Atmos.* **123**, 6804–6821 (2018).
49. Komatsu, K. K., Alexeev, V. A., Repina, I. A. & Tachibana, Y. Poleward upgliding Siberian atmospheric rivers over sea ice heat up arctic upper air. *Sci. Rep.* **8**, 2872 (2018).
50. Hegyi, B. M. & Taylor, P. C. The unprecedented 2016–2017 Arctic sea ice growth season: the crucial role of atmospheric rivers and longwave fluxes. *Geophys. Res. Lett.* **45**, 5204–5212 (2018).
51. Wille, J. D. et al. West Antarctic surface melt triggered by atmospheric rivers. *Nat. Geosci.* **12**, 911–916 (2019).
52. Dettinger, M. D. Climate change, atmospheric rivers, and floods in California – a multimodel analysis of storm frequency and magnitude changes. *J. Am. Water Resour. Assoc.* **47**, 514–523 (2011).
53. Ralph, F. M., Coleman, T. A., Neiman, P. J., Zamora, R. J. & Dettinger, M. D. Observed impacts of duration and seasonality of atmospheric river landfalls on soil moisture and runoff in coastal northern California. *J. Hydrometeorol.* **14**, 443–459 (2013).
54. Ralph, F. M. et al. A scale to characterize the strength and impacts of atmospheric rivers. *Bull. Am. Meteorol. Soc.* **100**, 269–289 (2019).
55. Payne, A. E. & Magnusdottir, G. Dynamics of landfalling atmospheric rivers over the North Pacific in 30 years of MERRA reanalysis. *J. Clim.* **27**, 7133–7150 (2014).
56. Fish, M. A., Wilson, A. M. & Raph, F. M. Atmospheric river families: definition and associated synoptic conditions. *J. Hydrometeorol.* **20**, 2091–2108 (2019).
57. White, A. B., Moore, B. J., Gottas, D. J. & Neiman, P. J. Winter storm conditions leading to excessive runoff above California's Oroville Dam during January and February 2017. *Bull. Am. Meteorol. Soc.* **100**, 55–70 (2019).
58. Hendy, I. L., Napier, T. J. & Schimmelmann, A. From extreme rainfall to drought: 250 years of annually resolved sediment deposition in Santa Barbara Basin, California. *Quat. Int.* **387**, 3–12 (2015).
59. Du, X., Hendy, I. & Schimmelmann, A. A 9000-year flood history for Southern California: a revised stratigraphy of varved sediments in Santa Barbara Basin. *Mar. Geol.* **397**, 29–42 (2018).
60. Gonzales, K. R., Swain, D. L., Nardi, K. M., Barnes, E. A. & Diffenbaugh, N. S. Recent warming of landfalling atmospheric rivers along the west coast of the United States. *J. Geophys. Res. Atmos.* **124**, 6810–6826 (2019).
61. Siler, N. & Roe, G. How will orographic precipitation respond to surface warming? An idealized thermodynamic perspective. *Geophys. Res. Lett.* **41**, 2606–2613 (2014).
62. O'Gorman, P. A. & Schneider, T. The physical basis for increases in precipitation extremes in simulations of 21st-century climate change. *Proc. Natl Acad. Sci. USA* **106**, 14773–14777 (2009).
63. Kirshbaum, D. J. & Smith, R. B. Orographic precipitation in the tropics: large-eddy simulations and theory. *J. Atmos. Sci.* **66**, 2559–2578 (2009).
64. Gao, Y. et al. Dynamical and thermodynamical modulations on future changes of landfalling atmospheric rivers over western North America. *Geophys. Res. Lett.* **42**, 7179–7186 (2015).
65. Lavers, D. A. et al. Future changes in atmospheric rivers and their implications for winter flooding in Britain. *Environ. Res. Lett.* **8**, 034010 (2013).
66. Gao, Y., Lu, J. & Leung, L. R. Uncertainties in projecting future changes in atmospheric rivers and their impacts on heavy precipitation over Europe. *J. Clim.* **29**, 6711–6726 (2016).
67. Kaplan, M. et al. The role of upstream mid-tropospheric circulations in the Sierra Nevada enabling leeside (spillover) precipitation. Part II: A secondary atmospheric river accompanying a midlevel jet. *J. Hydrometeorol.* **10**, 1327–1354 (2009).
68. Backes, T., Kaplan, M. L., Schumer, R. & Mejia, J. F. A climatology of the vertical structure of water vapor transport to the Sierra Nevada in cool season atmospheric river precipitation events. *J. Hydrometeorol.* **16**, 1029–1047 (2015).

69. Shepherd, T. G. Atmospheric circulation as a source of uncertainty in climate change projections. *Nat. Geosci.* **7**, 703–708 (2014).
70. Vallis, G. K., Zurita-Gotor, P., Cairns, C. & Kidston, J. Response of the large-scale structure of the atmosphere to global warming. *Q. J. R. Meteorol. Soc.* **141**, 1479–1501 (2015).
71. Butler, A. H., Thompson, D. W. J. & Heikes, R. The steady-state atmospheric circulation response to climate change–like thermal forcings in a simple general circulation model. *J. Clim.* **23**, 3474–3496 (2010).
72. Screen, J. A. & Simmonds, I. The central role of diminishing sea ice in recent Arctic temperature amplification. *Nature* **464**, 1334–1337 (2010).
73. Stuecker, M. F. et al. Polar amplification dominated by local forcing and feedbacks. *Nat. Clim. Change* **8**, 1076–1081 (2018).
74. Held, I. M. Large-scale dynamics and global warming. *Bull. Am. Meteorol. Soc.* **74**, 228–242 (1993).
75. Shaw, T. & Voigt, A. Tug of war on summertime circulation between radiative forcing and sea-surface warming. *Nat. Geosci.* **8**, 560–566 (2015).
76. Deser, C., Tomas, R. A. & Sun, L. The role of ocean–atmosphere coupling in the zonal-mean atmospheric response to Arctic sea ice loss. *J. Clim.* **28**, 2168–2186 (2015).
77. Barnes, E. A. & Screen, J. A. The impact of Arctic warming on the midlatitude jet-stream: Can it? Has it? Will it? *WIREs Clim. Change* **6**, 277–286 (2015).
78. Barnes, E. A. & Polvani, L. Response of the midlatitude jets, and of their variability, to increased greenhouse gases in the CMIP5 models. *J. Clim.* **26**, 7117–7135 (2013).
79. Lu, J., Vecchi, G. A. & Reichler, T. Expansion of the Hadley cell under global warming. *Geophys. Res. Lett.* **34**, L06805 (2007).
80. Frierson, D. M. W., Lu, J. & Chen, G. Width of the Hadley cell in simple and comprehensive general circulation models. *Geophys. Res. Lett.* **34**, L06804 (2007).
81. Yin, J. H. A consistent poleward shift of the storm tracks in simulations of 21st century climate. *Geophys. Res. Lett.* **32**, L18701 (2005).
82. Chang, E. K. M., Guo, Y. & Xia, X. CMIP5 multimodel ensemble projection of storm track change under global warming. *J. Geophys. Res. Atmos.* **117**, D23118 (2012).
83. Willison, J., Robinson, W. A. & Lackmann, G. M. The importance of resolving mesoscale latent heating in the North Atlantic storm track. *J. Atmos. Sci.* **70**, 2234–2250 (2013).
84. Li, M., Woollings, T., Hodges, K. & Masato, G. Extratropical cyclones in a warmer, moister climate: A recent Atlantic analogue. *Geophys. Res. Lett.* **41**, 8594–8601 (2014).
85. Nusbaumer, J. & Noone, D. Numerical evaluation of the modern and future origins of atmospheric river moisture over the west coast of the United States. *J. Geophys. Res. Atmos.* **123**, 6423–6442 (2018).
86. Pendergrass, A. G. What precipitation is extreme? *Science* **360**, 1072 (2018).
87. O'Gorman, P. A. Precipitation extremes under climate change. *Curr. Clim. Change Rep.* **1**, 49–59 (2015).
88. Hagos, S. M., Leung, L. R., Yoon, J.-H., Lu, J. & Gao, Y. A projection of changes in landfalling atmospheric river frequency and extreme precipitation over western North America from the Large Ensemble CESM simulations. *Geophys. Res. Lett.* **43**, 1357–1363 (2016).
89. Benedict, I., Ødemark, K., Nipen, T. & Moore, R. Large-scale flow patterns associated with extreme precipitation and atmospheric rivers over Norway. *Mon. Weather Rev.* **147**, 1415–1428 (2019).
90. Guan, B., Molotch, N. P., Waliser, D. E., Fetzer, E. J. & Neiman, P. J. Extreme snowfall events linked to atmospheric rivers and surface air temperature via satellite measurements. *Geophys. Res. Lett.* **37**, L20401 (2010).
91. Smith, B. L., Yuter, S. E., Neiman, P. J. & Kingsmill, D. E. Water vapor fluxes and orographic precipitation over northern California associated with a landfalling atmospheric river. *Mon. Weather. Rev.* **138**, 74–100 (2010).
92. Hecht, C. W. & Cordeira, J. M. Characterizing the influence of atmospheric river orientation and intensity on precipitation distributions over North Coastal California. *Geophys. Res. Lett.* **44**, 9048–9058 (2017).
93. Valenzuela, R. A. & Garreaud, R. D. Extreme daily rainfall in central-southern Chile and its relationship with low-level horizontal water vapor fluxes. *J. Hydrometeorol.* **20**, 1829–1850 (2019).
94. Westra, S., Alexander, L. V. & Zwiers, F. W. Global increasing trends in annual maximum daily precipitation. *J. Clim.* **26**, 3904–3918 (2013).
95. Liu, C. et al. Continental-scale convection-permitting modeling of the current and future climate of North America. *Clim. Dyn.* **49**, 71–95 (2017).
96. Shi, X. & Durran, D. R. The response of orographic precipitation over idealized midlatitude mountains due to global increases in CO_2. *J. Clim.* **27**, 3938–3956 (2014).
97. Pavelsky, T. M., Sobolowski, S., Kapnick, S. B. & Barnes, J. B. Changes in orographic precipitation patterns caused by a shift from snow to rain. *Geophys. Res. Lett.* **39**, L18706 (2012).
98. Sandvik, M. I., Sorteberg, A. & Rasmussen, R. Sensitivity of historical orographically enhanced extreme precipitation events to idealized temperature perturbations. *Clim. Dyn.* **50**, 143–157 (2018).
99. Haarsma, R. J. et al. High resolution model intercomparison project (HighResMIP v1.0) for CMIP6. *Geosci. Model Dev.* **9**, 4185–4208 (2016).
100. Mahoney, K. et al. An examination of an inland-penetrating atmospheric river flood event under potential future thermodynamic conditions. *J. Clim.* **31**, 6281–6297 (2018).
101. Shi, X. & Durran, D. Sensitivities of extreme precipitation to global warming are lower over mountains than over oceans and plains. *J. Clim.* **29**, 4779–4791 (2016).
102. Swain, D. L., Langenbrunner, B., Neelin, J. D. & Hall, A. Increasing precipitation volatility in twenty-first-century California. *Nat. Clim. Change* **8**, 427–433 (2018).
103. Gershunov, A., Shulgina, T., Ralph, F. M., Lavers, D. A. & Rutz, J. J. Assessing the climate-scale variability of atmospheric rivers affecting western North America. *Geophys. Res. Lett.* **44**, 7900–7908 (2017).
104. Sharma, A., Wasko, C. & Lettenmaier, D. P. If precipitation extremes are increasing, why aren't floods? *Water Resour. Res.* **54**, 8545–8551 (2018).
105. Wang, G., Power, S. B. & McGree, S. Unambiguous warming in the western tropical Pacific primarily caused by anthropogenic forcing. *Int. J. Climatol.* **36**, 933–944 (2016).
106. Sharma, A. R. & Děry, S. J. Variability and trends of landfalling atmospheric rivers along the Pacific Coast of northwestern North America. *Int. J. Climatol.* **40**, 544–558 (2020).
107. Espinoza, V., Waliser, D. E., Guan, B., Lavers, D. A. & Ralph, F. M. Global analysis of climate change projection effects on atmospheric rivers. *Geophys. Res. Lett.* **45**, 4299–4308 (2018).
108. Payne, A. E. & Magnusdottir, G. An evaluation of atmospheric rivers over the North Pacific in CMIP5 and their response to warming under RCP 8.5. *J. Geophys. Res. Atmos.* **120**, 11173–11190 (2015).
109. Radić, V., Cannon, A. J., Menounos, B. & Gi, N. Future changes in autumn atmospheric river events in British Columbia, Canada, as projected by CMIP5 global climate models. *J. Geophys. Res. Atmos.* **120**, 9279–9302 (2015).
110. Shields, C. A. & Kiehl, J. T. Atmospheric river landfall-latitude changes in future climate simulations. *Geophys. Res. Lett.* **43**, 8775–8782 (2016).
111. Shields, C. A. & Kiehl, J. T. Simulating the pineapple express in the half degree community climate system model, CCSM4. *Geophys. Res. Lett.* **43**, 7767–7773 (2016).
112. Sousa, P. M., Blamey, R. C., Reason, C. J. C., Ramos, A. M. & Trigo, R. M. The 'Day Zero' Cape Town drought and the poleward migration of moisture corridors. *Environ. Res. Lett.* **13**, 124025 (2018).
113. Warner, M. D., Mass, C. F. & Salathé, E. P. Jr. Changes in winter atmospheric rivers along the North American west coast in CMIP5 climate models. *J. Hydrometeorol.* **16**, 118–128 (2015).
114. Polade, S. D., Gershunov, A., Cayan, D. R., Dettinger, M. D. & Pierce, D. W. Precipitation in a warming world: Assessing projected hydro-climate changes in California and other Mediterranean climate regions. *Sci. Rep.* **7**, 10783 (2017).
115. Sousa, P. M. et al. North Atlantic integrated water vapor transport–from 850 to 2100 CE: impacts on western European rainfall. *J. Clim.* **33**, 263–279 (2020).
116. Dong, L., Leung, L. R. & Song, F. Future changes of subseasonal precipitation variability in North America during winter under global warming. *Geophys. Res. Lett.* **45**, 12467–12476 (2018).
117. Dong, L., Leung, L. R., Lu, J. & Gao, Y. Contributions of extreme and non-extreme precipitation to California precipitation seasonality changes under warming. *Geophys. Res. Lett.* **46**, 13470–13478 (2019).
118. Paltan, H. et al. Global floods and water availability driven by atmospheric rivers. *Geophys. Res. Lett.* **44**, 10387–10395 (2017).
119. Barth, N. A., Villarini, G. & White, K. Accounting for mixed populations in flood frequency analysis: a Bulletin 17C perspective. *J. Hydrol. Eng.* **24**, 04019002 (2019).
120. Barth, N. A., Villarini, G., Nayak, M. A. & White, K. Mixed populations and annual flood frequency estimates in the western United States: the role of atmospheric rivers. *Water Resour. Res.* **53**, 257–269 (2017).
121. Ralph, F. M. et al. Flooding on California's Russian River: role of atmospheric rivers. *Geophys. Res. Lett.* **33**, L13801 (2006).
122. Neiman, P. J., Schick, L. J., Ralph, F. M., Hughes, M. & Wick, G. A. Flooding in western Washington: the connection to atmospheric rivers. *J. Hydrometeorol.* **12**, 1337–1358 (2011).
123. Khouakhi, A. & Villarini, G. On the relationship between atmospheric rivers and high sea water levels along the US West Coast. *Geophys. Res. Lett.* **43**, 8815–8822 (2016).
124. Demaria, E. M. C. et al. Observed hydrologic impacts of landfalling atmospheric rivers in the Salt and Verde river basins of Arizona, United States. *Water Resour. Res.* **53**, 10025–10042 (2017).
125. Nayak, M.A. & Villarini, G. A long-term perspective of the hydroclimatological impacts of atmospheric rivers over the central United States. *Water Resour. Res.* **53**, 1144–1166. (2017).
126. Dirmeyer, P. A. & Kinter, J. L. III The "maya express": floods in the US Midwest. *EOS Trans.* **90**, 101–102 (2009).
127. Moore, B. J., Neiman, P. J., Ralph, F. M. & Barthold, F. E. Physical processes associated with heavy flooding rainfall in Nashville, Tennessee, and vicinity during 1–2 May 2010: the role of an atmospheric river and mesoscale convective systems. *Mon. Weather. Rev.* **140**, 358–378 (2012).
128. Azad, R. & Sorteberg, A. Extreme daily precipitation in coastal western Norway and the link to atmospheric rivers. *J. Geophys. Res. Atmos.* **122**, 2080–2095 (2017).
129. Ramos, A. M., Martins, M. J., Tomé, R. & Trigo, R. M. Extreme precipitation events in summer in the Iberian Peninsula and its relationship with atmospheric rivers. *Front. Earth Sci.* **6**, 110 (2018).
130. Zscheischler, J. et al. Future climate risk from compound events. *Nat. Clim. Change* **8**, 469–477 (2018).
131. Rössler, O. et al. Retrospective analysis of a nonforecasted rain-on-snow flood in the Alps – a matter of model limitations or unpredictable nature? *Hydrol. Earth Syst. Sci.* **18**, 2265–2285 (2014).
132. Oakley, N. S., Lancaster, J. T., Kaplan, M. L. & Ralph, F. M. Synoptic conditions associated with cool season post-fire debris flows in the Transverse Ranges of southern California. *Nat. Hazards* **88**, 327–354 (2017).
133. Oakley, N. S. et al. A 22-year climatology of cool season hourly precipitation thresholds conducive to shallow landslides in California. *Earth Interact.* **22**, 1–35 (2018).
134. Dettinger, M. D. Atmospheric rivers as drought busters on the US West Coast. *J. Hydrometeorol.* **14**, 1721–1732 (2013).
135. Wang, S. Y. S., Yoon, J.-H., Becker, E. & Gillies, R. California from drought to deluge. *Nat. Clim. Change* **7**, 465–468 (2017).
136. Hu, H., Dominguez, F., Kumar, P., McDonnell, J. & Gochis, D. A numerical water tracer model for understanding event-scale hydrometeorological phenomena. *J. Hydrometeorol.* **19**, 947–967 (2018).
137. Leung, L. R. & Qian, Y. Atmospheric rivers induced heavy precipitation and flooding in the western US simulated by the WRF regional climate model. *Geophys. Res. Lett.* **36**, L03820 (2009).
138. Guan, B., Waliser, D. E., Ralph, F. M., Fetzer, E. J. & Neiman, P. J. Hydrometeorological characteristics of rain-on-snow events associated with atmospheric rivers. *Geophys. Res. Lett.* **43**, 2964–2973 (2016).
139. Chen, X., Leung, L. R., Wigmosta, M. & Richmond, M. Impact of atmospheric rivers on surface hydrological processes in western US watersheds. *J. Geophys. Res. Atmos.* **124**, 8896–8916 (2019).
140. Leung, L. R. et al. Mid-century ensemble regional climate change scenarios for the western United States. *Clim. Change* **62**, 75–113 (2004).

141. Barnett, T. P., Adam, J. C. & Lettenmaier, D. P. Potential impacts of a warming climate on water availability in snow-dominated regions. *Nature* **438**, 303–309 (2005).
142. Rauscher, S. A., Pal, J. S., Diffenbaugh, N. S. & Benedetti, M. M. Future changes in snowmelt-driven runoff timing over the western US. *Geophys. Res. Lett.* **35**, L16703 (2008).
143. Gobiet, A. et al. 21st century climate change in the European Alps - a review. *Sci. Total. Environ.* **493**, 1138–1151 (2014).
144. Musselman, K. N., Clark, M. P., Liu, C., Ikeda, K. & Rasmussen, R. Slower snowmelt in a warmer world. *Nat. Clim. Change* **7**, 214–219 (2017).
145. Cohen, J., Ye, H. & Jones, J. Trends and variability in rain-on-snow events. *Geophys. Res. Lett.* **42**, 7115–7122 (2015).
146. Musselman, K. N. et al. Projected increases and shifts in rain-on-snow flood risk over western North America. *Nat. Clim. Change* **8**, 808–812 (2018).
147. Huang, X., Hall, A. D. & Berg, N. Anthropogenic warming impacts on today's Sierra Nevada snowpack and flood risk. *Geophys. Res. Lett.* **45**, 6215–6222 (2018).
148. Islam, S. U., Curry, C. L., Déry, S. J. & Zwiers, F. W. Quantifying projected changes in runoff variability and flow regimes of the Fraser River Basin, British Columbia. *Hydrol. Earth Syst. Sci.* **23**, 811–828 (2019).
149. Curry, C. L., Islam, S. U., Zwiers, F. W. & Déry, S. J. Atmospheric rivers increase future flood risk in Western Canada's largest pacific river. *Geophys. Res. Lett.* **46**, 1651–1661 (2019).
150. Singh, I., Dominguez, F., Demaria, E. & Walter, J. Extreme landfalling atmospheric river events in Arizona: Possible future changes. *J. Geophys. Res. Atmos.* **123**, 7076–7097 (2018).
151. Hu, H. et al. Linking atmospheric river hydrological impacts on the US West Coast to Rossby wave breaking. *J. Clim.* **30**, 3381–3399 (2017).
152. Corringham, T. W., Ralph, F. M., Gershunov, A., Cayan, D. R. & Talbot, C. A. Atmospheric rivers drive flood damages in the western United States. *Sci. Adv.* **5**, eaax4631 (2019).
153. Hatchett, B. J. et al. Avalanche fatalities during atmospheric river events in the western United States. *J. Hydrometeorol.* **18**, 1359–1374 (2017).
154. Dominguez, F. et al. Tracking an atmospheric river in a warmer climate: from water vapor to economic impacts. *Earth Syst. Dyn.* **9**, 249–266 (2018).
155. Shields, C. A. et al. Atmospheric river tracking method intercomparison project (ARTMIP): project goals and experimental design. *Geosci. Model Dev.* **11**, 2455–2474 (2018).
156. Rutz, J. J. et al. The atmospheric river tracking method intercomparison project (ARTMIP): quantifying uncertainties in atmospheric river climatology. *J. Geophys. Res. Atmos.* **124**, 13777–13802 (2019).
157. Delworth, T. L. et al. Simulated climate and climate change in the GFDL CM2.5 high-resolution coupled climate model. *J. Clim.* **25**, 2755–2781 (2012).
158. Kinter, J. L. et al. Revolutionizing climate modeling with Project Athena: a multi-institutional, international collaboration. *Bull. Am. Meteorol. Soc.* **94**, 231–245 (2013).
159. Mizielinski, M. S. et al. High resolution global climate modelling; the UPSCALE project, a large simulation campaign. *Geosci. Model Dev.* **7**, 1629–1640 (2014).
160. Small, R. J. et al. A new synoptic scale resolving global climate simulation using the Community Earth System Model. *J. Adv. Modeling Earth Syst.* **6**, 1065–1094 (2014).
161. Wehner, M. F. et al. The effect of horizontal resolution on simulation quality in the community atmospheric model, CAM5.1. *J. Adv. Model. Earth Syst.* **6**, 980–997 (2014).
162. Kamae, Y., Mei, W. & Xie, S.-P. Ocean warming pattern effects on future changes in East Asian atmospheric rivers. *Environ. Res. Lett.* **14**, 054019 (2019).
163. Hagos, S., Leung, L. R., Yang, Q., Zhao, C. & Lu, J. Resolution and dynamical core dependence of atmospheric river frequency in global model simulations. *J. Clim.* **28**, 2764–2776 (2015).
164. Guan, B. & Waliser, D. E. Atmospheric rivers in 20 year weather and climate simulations: A multimodel, global evaluation. *J. Geophys. Res. Atmos.* **122**, 5556–5581 (2017).
165. Roberts, M. J. et al. The benefits of global high resolution for climate simulation: process understanding and the enabling of stakeholder decisions at the regional scale. *Bull. Am. Meteorol. Soc.* **99**, 2341–2359 (2018).
166. Roberts, M. J. et al. Description of the resolution hierarchy of the global coupled HadGEM3-GC3.1 model as used in CMIP6 HighResMIP experiments. *Geosci. Model Dev.* **12** 4999–5028 (2019).
167. Roberts, M. MOHC HadGEM3-GC31-HM model output prepared for CMIP6 HighResMIP hist-1950. Version YYYYMMDD. *Earth Syst. Grid Federation*, https://doi.org/10.22033/ESGF/CMIP6.6040 (2018).
168. Demory, M.-E. et al. The role of horizontal resolution in simulating drivers of the global hydrological cycle. *Clim. Dyn.* **42**, 2201–2225 (2014).
169. Lu, J. et al. Toward the dynamical convergence on the jet stream in aquaplanet AGCMs. *J. Clim.* **28**, 6763–6782 (2015).
170. Vannière, B. et al. Multi-model evaluation of the sensitivity of the global energy budget and hydrological cycle to resolution. *Clim. Dyn.* **52**, 6817–6846 (2019).
171. van Haren, R., Haarsma, R. J., van Oldenborgh, G. J. & Hazeleger, W. Resolution dependence of European precipitation in a state-of-the-art atmospheric general circulation model. *J. Clim.* **28**, 5134–5149 (2015).
172. Schiemann, R. et al. Mean and extreme precipitation over European river basins better simulated in a 25km AGCM. *Hydrol. Earth Syst. Sci.* **22**, 3933–3950 (2018).
173. Goldenson, N., Leung, L. R., Bitz, C. M. & Blanchard-Wrigglesworth, E. Influence of atmospheric rivers on mountain snowpack in the western United States. *J. Clim.* **31**, 9921–9940 (2018).
174. Mundhenk, B. D., Barnes, E. A., Maloney, E. D. & Baggett, C. F. Skillful empirical subseasonal prediction of landfalling atmospheric river activity using the Madden–Julian oscillation and quasi-biennial oscillation. *npj Clim. Atmos. Sci.* **1**, 20177 (2018).
175. Richter, J. H., Solomon, A. & Bacmeister, J. T. On the simulation of the quasi-biennial oscillation in the Community Atmosphere Model, version 5. *J. Geophys. Res. Atmos.* **119**, 3045–3062 (2014).
176. Stone, D. A. et al. Experiment design of the International CLIVAR C20C+ Detection and Attribution project. *Weather Clim. Extremes* **24**, 100206 (2019).
177. Gershunov, A. et al. Precipitation regime change in Western North America: the role of atmospheric rivers. *Sci. Rep.* **9**, 9944 (2019).
178. Mallakpour, I., Sadegh, M. & AghaKouchak, A. A new normal for streamflow in California in a warming climate: wetter wet seasons and drier dry seasons. *J. Hydrol.* **567**, 203–211 (2018).
179. Pierce, D. W. et al. The key role of heavy precipitation events in climate model disagreements of future annual precipitation changes in California. *J. Clim.* **26**, 5879–5896 (2013).
180. Loikith, P. C. et al. A climatology of daily synoptic circulation patterns and associated surface meteorology over southern South America. *Clim. Dyn.* **53**, 4019–4035 (2019).
181. Pasquier, J. T., Pfahl, S. & Grams, C. M. Modulation of atmospheric river occurrence and associated precipitation extremes in the North Atlantic Region by European weather regimes. *Geophys. Res. Lett.* **46**, 1014–1023 (2019).
182. Lavers, D. A., Ralph, F. M., Waliser, D. E., Gershunov, A. & Dettinger, M. D. Climate change intensification of horizontal water vapor transport in CMIP5. *Geophys. Res. Lett.* **42**, 5617–5625 (2015).
183. Mattingly, K. S., Ramseyer, C. A., Rosen, J. J., Mote, T. L. & Muthyala, R. Increasing water vapor transport to the Greenland Ice Sheet revealed using self-organizing maps. *Geophys. Res. Lett.* **43**, 9250–9258 (2016).

Acknowledgements

L.R.L. and C.A.S. (NCAR via NSF IA 1947282) are supported by the U.S. Department of Energy Office of Science Biological and Environmental Research as part of the Earth and Environmental System Modeling Regional and Global Model Analysis program area. Pacific Northwest National Laboratory is operated for the Department of Energy by Battelle Memorial Institute under contract DE-AC05-75RL01830. The National Center for Atmospheric Research (NCAR) is sponsored by the National Science Foundation (NSF) under Cooperative Agreement 1852977. G.V. is supported by the U.S. Army Corps of Engineers' Institute for Water Resources. A.M.R. is supported by the Scientific Employment Stimulus 2017 from FCT (CEECIND/00027/2017). Atmospheric River Tracking Method Intercomparison Project (ARTMIP) is a grass-roots community effort and has received support from the U.S. Department of Energy Office of Science Biological and Environmental Research as part of the Regional and Global Climate Modeling Program, and the Center for Western Weather and Water Extremes at Scripps Institute for Oceanography at the University of California, San Diego.

Author contributions

The authors all contributed equally to the identification of main topics and their organization in the article. A. E. Payne led the writing and revision of the manuscript, with input and contributions from N. Siler (theory), L. R. Leung (theory, impacts), A. M. Ramos (projections), G. Villarini (impacts), C. A. Shields (Box 1) and M.-E. Demory (Box 2). A. E. Payne directed the modification of Fig. 1 and designed Figs. 2 and 3. C. A. Shields contributed the figure in Box 1 and M.-E. Demory contributed the figure in Box 2.

Competing interests

The authors declare no competing interests.

Peer review information

Nature Reviews Earth & Environment thanks Y. Kamae, F. Dominguez, V. Espinoza and M. Nayak for their contribution to the peer review of this work.

Publisher's note

Springer Nature remains neutral with regard to jurisdictional claims in published maps and institutional affiliations.

Supplementary information

Supplementary information is available for this paper at https://doi.org/10.1038/s43017-020-0030-5.